Metal-insulator transition in $TlSr_2CoO_5$ from orbital degeneracy and spin disproportionation

D. Foerster
CPTMB, Université de Bordeaux I, 33405 Talence, France

R. Hayn
Institut für Festkörper- und Werkstofforschung (IFW), 01171 Dresden, Germany

T. Pruschke and M. Zölfl
Institut für Theoretische Physik, Universität Regensburg, 93040 Regensburg, Germany

H. Rosner
Department of Physics, University of California, 95616 Davis, California

(Received 9 October 2000; revised manuscript received 23 March 2001; published 19 July 2001)

To describe the metal-insulator transition in the oxide $TlSr_2CoO_5$, we investigate the electronic structure of its high-temperature tetragonal phase by the local density approximation (LDA) and model Hartree-Fock calculations. Within the LDA we find a homogeneous metallic and ferromagnetic ground state; however, when including the strong Coulomb interaction in the $3d$ shell more explicitly within the Hartree-Fock approximation, we find an insulating state of lower energy that exhibits both spin and orbital order. The instability of the metallic state toward the insulating one is driven by orbital degeneracy and a near degeneracy in energy of states of intermediate ($s=1$) and high ($s=2$) spin. We also interpret our results in terms of a simple model.

DOI: 10.1103/PhysRevB.64.075104 PACS number(s): 71.30.+h, 71.20.−b, 71.15.Mb

INTRODUCTION

Six years ago, the observation of colossal magnetoresistance in doped manganites lead to a renewed interest in transition-metal oxides, see Ref. 1 for a review. These materials often exhibit complex phases with coexisting magnetic and orbital[2] orders and with Jahn-Teller-like distortions. The origin of this complexity is the subtle interplay between different types of local Coulomb interactions within their $3d$ electronic orbitals.

The Co^{3+} analog $TlSr_2CoO_5$ of nonsuperconducting $TlSr_2CuO_5$ is a recent addition to this class of materials. It is of perovskite structure, with a first-order transition at ≈ 310 K from a tetragonal and metallic phase, with a ferromagnetic Curie-like susceptibility at high temperature to an orthorhombic and insulating phase with two crystallographically inequivalent Co sites. The magnetic structure below 310 K is complicated, exhibiting both ferromagnetic and antiferromagnetic correlations; below $T \approx 150$ K, antiferromagnetic long-range order sets in.[3] The special interest in this oxide is due to its quasi-two-dimensional (2D) character and, from the point of view of applications, it may be useful that the metal-insulator transition in the oxide occurs at room temperature.

In this paper we explain the 310-K metal-insulator transition of $TlSr_2CoO_5$ in terms of an instability of its high-temperature electronic structure. We show that the homogeneous ground state can lower its energy by breaking orbital degeneracy and by simultaneously acquiring both orbital and spin order. It should be noted, however, that the instability of the high-temperature phase that we found is toward a phase that differs in details from the one seen experimentally.

METHOD OF ANALYSIS

A. Band-structure calculation

We start with a density-functional band-structure calculation in the high-temperature phase, using the local-density approximation (LDA) for the exchange and correlation potential; see Ref. 4 for a review. Above a transition temperature of 310 K, the crystal structure is tetragonal, with a $P4/mmm$ space group (see Fig. 1). As input parameters of the calculation, we used experimentally determined lattice parameters of $a=0.375$ nm, $c=0.877$ nm, and relative strontium and apex oxygen (03) positions (that are not fixed by the space group) of $z=0.2903$ and 0.2330, respectively.[3] We employed a recently developed full-potential nonorthogonal local-orbital (FPLO) minimum basis scheme[5] that imposes no shape restriction on the potential. The calculation was scalar relativistic, with the spatial extent of the basis orbitals controlled by a confining potential of $(r/r_0)^4$ that was optimized with respect to the total energy. The thallium $\{5s,5p,5d,6s,6p\}$, strontium $\{4s,4p,5s,5p,5d\}$, cobalt $\{3s,3p,4s,4p,3d\}$, and oxygen $\{2s,2p,3d\}$ orbitals were treated as valence orbitals, while the lower-lying orbitals were treated as core states. The inclusion of Tl $\{5s,5p,5d\}$, Sr $\{4s,4p\}$, and Co $\{3s,3p\}$ states in the valence states was necessary to account for non-negligible core-core overlaps. The O $3d$ states were taken into account to increase the completeness of the basis set. The results of this LDA calculation will be discussed in detail further below.

B. Tight-binding Hartree-Fock calculation

To take into account the strong Coulomb interactions in the Co d shell more accurately we could have used the

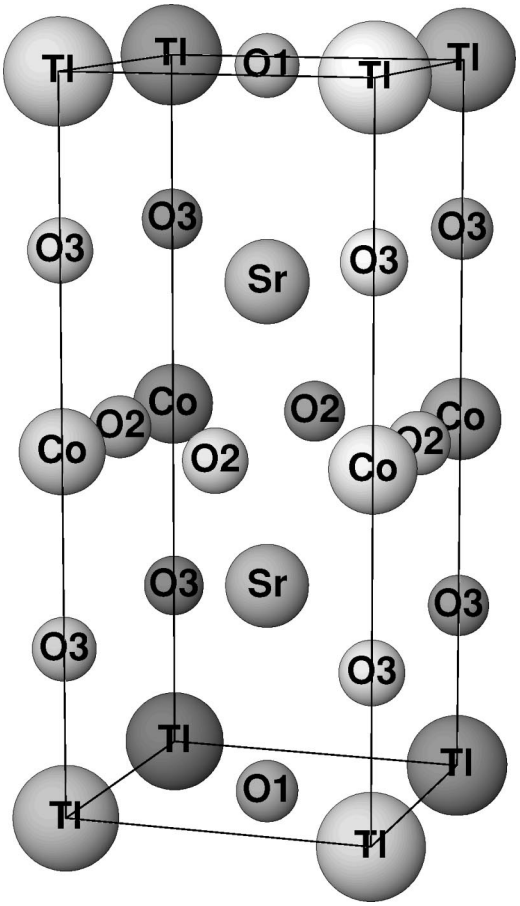

FIG. 1. Crystal structure of the high-temperature tetragonal phase of $TlSr_2CoO_5$.

LDA+U approach described in detail in Ref. 6. Instead, and in order to gain a more direct insight into the mechanism of the metal insulator transition at work, we included the Coulomb interactions in a minimal tight-binding Hamiltonian of all cobalt $3d$ and oxygen $2p$ orbitals in the CoO_2 plane, and used the results of the previously described LDA calculation to determine the hopping parameters of this model (see Ref. 7 for similar work). According to Koster-Slater-type symmetry considerations,[8] the overlap between the d and p orbitals may be parametrized in terms of two parameters which we denote as t_{e_g} and $t_{t_{2g}}$, respectively. Due to the perovskite structure, there is no direct Co-Co hopping, and we assume the absence of direct O-O hopping. With these approximations, the transfer-matrix elements for the planar Co-O bond in the x direction are

$$t_{dp}(\vec{x})=\begin{pmatrix} 0 & t_{t_{2g}} & 0 \\ 0 & 0 & 0 \\ 0 & 0 & t_{t_{2g}} \\ -\frac{1}{2}t_{e_g} & 0 & 0 \\ \frac{\sqrt{3}}{2}t_{e_g} & 0 & 0 \end{pmatrix}, \tag{1}$$

where the d and p orbitals are ordered as $d=\{d_{xy},d_{yz},d_{zx},d_{z^2},d_{x^2-y^2}\}$ and $p=\{p_x^{\vec{x}},p_y^{\vec{x}},p_z^{\vec{x}}\}$, respectively. The superscript $\vec{x}$ for the p orbitals indicates that they belong to the oxygen at $\frac{1}{2}a\vec{e}_x$, and the corresponding matrix for the Co-O bond in the y direction is obtained by formally interchanging $x\leftrightarrow y$ in the above table. The results of the band-structure calculation also determine the Co d-shell crystal-field parameters ϵ_i, $i=\{xy,yz,zx,z^2,x^2-y^2\}$ and the on-site energy ϵ_p of the oxygen p orbitals (we neglect the splitting of the oxygen p states due to tetragonal distortion). Tetragonal symmetry at the Co site leaves $\epsilon_{yz}=\epsilon_{zx}$ degenerate. The sum of the on-site energies and hopping amplitudes in the x and y directions defines the noninteracting part of a tight-binding model,

$$H=H_{tb}+H_{Coulomb},$$

$$H_{tb}=\sum_{i,j,\vec{R},\vec{R}',s} t_{ij}(\vec{R}-\vec{R}')a_{i,s}^{\dagger}(\vec{R})a_{j,s}(\vec{R}'), \tag{2}$$

where the orbital indices i and j range from 1 to 11 ($1\ldots5$ are the Co $3d$ orbitals), and s denotes the spin component. To complete the model, we add the local Coulomb energy at the Co sites as expressed in tight-binding orbitals:

$$H_{Coulomb}=\frac{1}{2}\sum_{i,j,k,l,s,s'} V_{ijkl}a_{i,s}^{\dagger}a_{j,s'}^{\dagger}a_{l,s'}a_{k,s}$$

with

$$V_{ijkl}=\left\langle ij\left|\frac{e^2}{|\vec{r}-\vec{r}'|}\right|kl\right\rangle. \tag{3}$$

To determine the V_{ijkl} coefficients, we use the rotational symmetry of the Coulomb interaction, and calculate related coefficients $\tilde{V}_{ijkl}$ in a spherical basis,[9]

$$\begin{aligned}\tilde{V}_{m_1m_2n_1n_2}&=\sum_{k=0}^{\infty}\frac{4\pi}{2k+1}\int dr_1dr_2\frac{r_<^k}{r_>^{k+1}}R_d^2(r_1)R_d^2(r_2)\\ &\times\int d\Omega_1Y_{2m_1}^*Y_{2n_1}Y_{km}\int d\Omega_2Y_{2m_2}^*Y_{2n_2}Y_{km}^*\\ &=25\sum_{k=0,2,4}(-1)^{m_1+n_2}F^{(k)}\begin{pmatrix}2&2&k\\0&0&0\end{pmatrix}^2\\ &\times\begin{pmatrix}2&2&k\\-m_1&n_1&m\end{pmatrix}\begin{pmatrix}2&2&k\\-n_2&m_2&m\end{pmatrix},\end{aligned}$$

$$F^{(0)}=A+\frac{7}{5}C,\quad F^{(2)}=49B+7C,\quad F^{(4)}=\frac{441}{35}C \tag{4}$$

and then transform $\tilde{V}$ to V in standard cubic orbitals.[10] In Eq. (4), $R_d(r)$ is the radial part of the $3d$ wave function, and to

obtain it we used formula C.16 of Ref. 11. $\{A,B,C\}$ are Racah's parametrization of the Slater integrals F^0, F^2, and F^4 as reviewed, e.g., in Ref. 9. Please note that expression (4) is rotationally invariant, and that all Coulomb interactions were included. Although we used the full expression for V_{ijkl} in our calculation, the Racah parameter B is rather small, and when it is taken to be zero we find a much simpler expression (in the cubic basis):

$$(V_{ijkl})_{B=0} = C(\delta_{ij}\delta_{kl} + \delta_{il}\delta_{jk}) + (A+C)\delta_{ik}\delta_{jl}. \quad (5)$$

Usually, one denotes the diagonal elements as $U = V_{iiii} = A + 3C$, and the Coulomb repulsion between different $(i \neq j)$ orbitals $V_{ijij} = A + C$ is smaller. From Eqs. (3) and (5), one finds the following expression for the Coulomb energy:

$$(H_{Coulomb})_{B=0} \doteq C\sum_{ij} P_i^+ P_j - C\sum_{ij} \vec{s}_i \cdot \vec{s}_j + \frac{2A+C}{4}\sum_{ij} n_i n_j, \quad (6)$$

with

$$n_i = a_{i,\uparrow}^+ a_{i,\uparrow} + a_{i,\downarrow}^+ a_{i,\downarrow} \quad \text{and} \quad P_i = a_{i,\uparrow} a_{i,\downarrow}$$

where the dot on the equal sign indicates that we ignore terms that merely redefine the chemical potential. The Coulomb energy can be given a more succinct and meaningful form by expressing it in terms of the total electronic spin $\vec{s}_{tot} = \Sigma_i \vec{s}_i$ and the total electronic charge $N = \Sigma_i n_i$ of all electron orbitals at a given site as follows:

$$(H_{Coulomb})_{B=0} \doteq J_H[D - (\vec{s}_{tot})^2] + \frac{\tilde{U}N^2}{2} + (\text{nondiagonal pairs}), \quad (7)$$

where $\tilde{U} = A + C/2$, $J_H = C$, and D counts the number of pairs on the same d orbital, $D = \Sigma_i P_i^+ P_i$, while the nondiagonal pairs $\Sigma_{i \neq j} P_i^+ P_j$ were omitted as their matrix elements are very small.

Treating the Coulomb interaction in an unrestricted Hartree-Fock (HF) approximation,[13] that allows for all spin- and charge-conserving correlations, gives the following renormalization of the on-site Hamilton matrix

$$\Delta t_{ij}^s = \sum_{l,m} V_{iljm} \sum_{s'} n_{lm}^{s'} - \sum_{l,m} V_{ilmj} n_{lm}^s, \quad (8)$$

where i and j denote the orbital indices of Co $3d$, and the density matrix

$$n_{lm}^s = \frac{1}{N_k}\sum_{k,\alpha}^{occ} \psi_l^{*\alpha s}(\vec{k})\psi_m^{\alpha s}(\vec{k}) \quad (9)$$

is calculated from the normalized wave functions $\psi_m^{\alpha s}(\vec{k})$, with band index α and momentum $\vec{k}$ (N_k corresponds to the number of k points). The total energy is given by

$$E = \langle H_{tb} \rangle + \langle H_{Coulomb} \rangle, \quad (10)$$

where

$$\langle H_{tb} \rangle = \frac{1}{N_k}\sum_{k,\alpha,s}^{occ} \sum_{l,m} \psi_l^{*\alpha s}(\vec{k}) t_{lm}(\vec{k}) \psi_m^{\alpha s}(\vec{k}) \quad (11)$$

is the mean (unrenormalized) kinetic energy, and

$$\langle H_{Coulomb} \rangle = \frac{1}{2}\sum_{m_1,m_2,m_3,m_4,s,s'} V_{m_1 m_2 m_3 m_4} n_{m_4 m_2}^s n_{m_3 m_1}^{s'} - \frac{1}{2}\sum_{m_1,m_2,m_3,m_4,s} V_{m_1 m_2 m_3 m_4} n_{m_4 m_1}^s n_{m_3 m_2}^s \quad (12)$$

is the interaction energy.

RESULTS

A. Full-potential local-orbital method

We performed two band-structure calculations, one spin symmetric (see Fig. 2) and the other one allowing for spin polarization (Fig. 3). Both solutions are metallic, but the magnetic one is energetically preferred by 0.54 eV per formula unit. The density of states (DOS) shows a high degree of covalency, such that part of the magnetic moment (calculated with all the overlap contributions) sits on oxygen ($m_O = 0.2\mu_B$), giving a total moment $m = 2.1\mu_B$ ($m_{Co} = 1.9\mu_B$). The corresponding occupation numbers are $n_{Co} = 7.2$ and $n_O = 5.1$.

The band structure of the nonmagnetic solution, together with the DOS for an easier identification of the structures, is shown in Fig. 4; the size of the dots included in the band structure in Fig. 4 symbolizes the relative cobalt $3d$ weight in the band. Evidently, the five bands crossing the Fermi level have predominantly Co $3d$ character. They hybridize quite strongly with $2p$ bands of the in-plane O(2), located at about 4–6 eV binding energy. The $2p$ bands of the other oxygens O(1) and O(3) are nonbonding, and located in between Co-$3d$ and O(2)-$2p$. The Co-$3d$ bands have only a small dispersion in the z direction (with the exception of Co $3d_{z^2}$), confirming the 2D character of the compound under consideration. We determined the energetic order of the $3d$ orbitals at the Γ point, because the effective d-d hybridization vanishes at this point in the tight-binding parametrization. We also analyzed the bands according to their predominant orbital character,[14] and found, in increasing order: d_{xy}, $d_{zx/yz}$, d_{z^2}, and $d_{x^2-y^2}$. Due to tetragonal symmetry, there is an exact degeneracy between the d_{zx} and d_{yz} orbital in the LDA calculation.

The ferromagnetic solution (Fig. 3) indicates a finite density of states of the majority spins at the Fermi surface. From this, we conclude that $TlSr_2CoO_5$ is not a half-metal, and that it may conduct electric current even in a spin-disordered

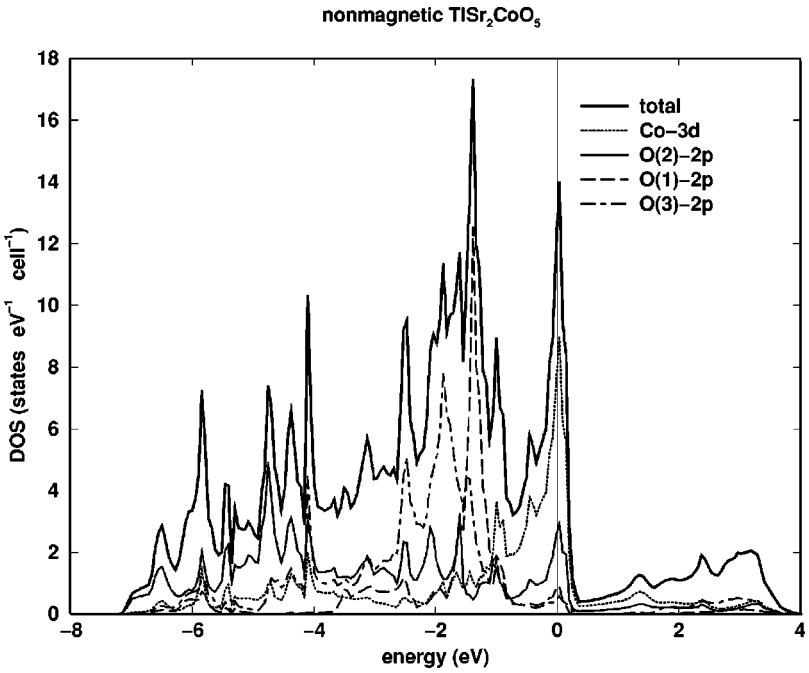

FIG. 2. Total and partial DOS of the nonmagnetic solution obtained using the full-potential nonorthogonal local-orbital (FPLO) method. The Fermi level is at zero energy.

phase. An orbital analysis (that is not documented here) shows that for a majority spin only $3d_{x^2-y^2}$ is partly occupied, while all the remaining majority bands ($3d_{xy}$, $3d_{zx/yz}$, $3d_{z^2}$) are completely below the Fermi level. For a minority spin, $3d_{xy}$, $3d_{zx/yz}$, and $3d_{z^2}$ are partly filled, whereas $3d_{x^2-y^2}$ is nearly empty. It is difficult to interpret such an itinerant ferromagnet in an ionic picture. But the value of its magnetic moment $m=2s\mu_B>2\mu_B$, indicates a state between intermediate ($s=1$) and high ($s=2$) spin.

B. Tight-binding Hartree-Fock calculation

To fix the parameters of the Hartree-Fock model, we compared its nonmagnetic HF solution with the five relevant bands of the FPLO result of the nonmagnetic LDA solution of Fig. 4. We estimated the crystal-field parameters to be (in eV) $\epsilon_{xy}=-1.0$, $\epsilon_{zx/yz}=-0.5$, $\epsilon_{z^2}=-0.2$, and $\epsilon_{x^2\text{-}y^2}=0.5$. The bandwidth determines the transfer terms $t_{e_g}=1.9$ and $t_{t_{2g}}=1.4$. The Racah parameters B and C are fixed to their ionic values for trivalent Co, as determined by infrared spectroscopy ($B=0.06$ and $C=0.46$),[15] whereas $A=2$ was chosen as a typical value for Co. The choice of ϵ_p depends on A due to the mean-field shift of the $3d$ level, and we used $\epsilon_p=11$ such that the position of the oxygen levels coincides with the O(2)-$2p$ position in the LDA. In fact, the position of the oxygen bands does not change very much for different Hartree-Fock solutions. The tight-binding bands resulting from these parameters are shown in Fig. 5, and agree reason-

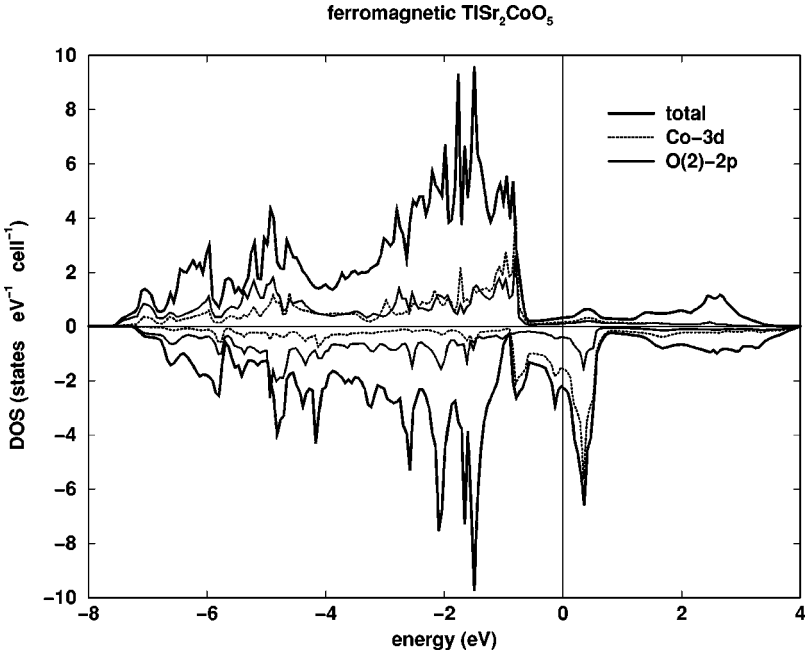

FIG. 3. Total and partial DOS of the ferromagnetic state of $TlSr_2CoO_5$ according to FPLO calculations.

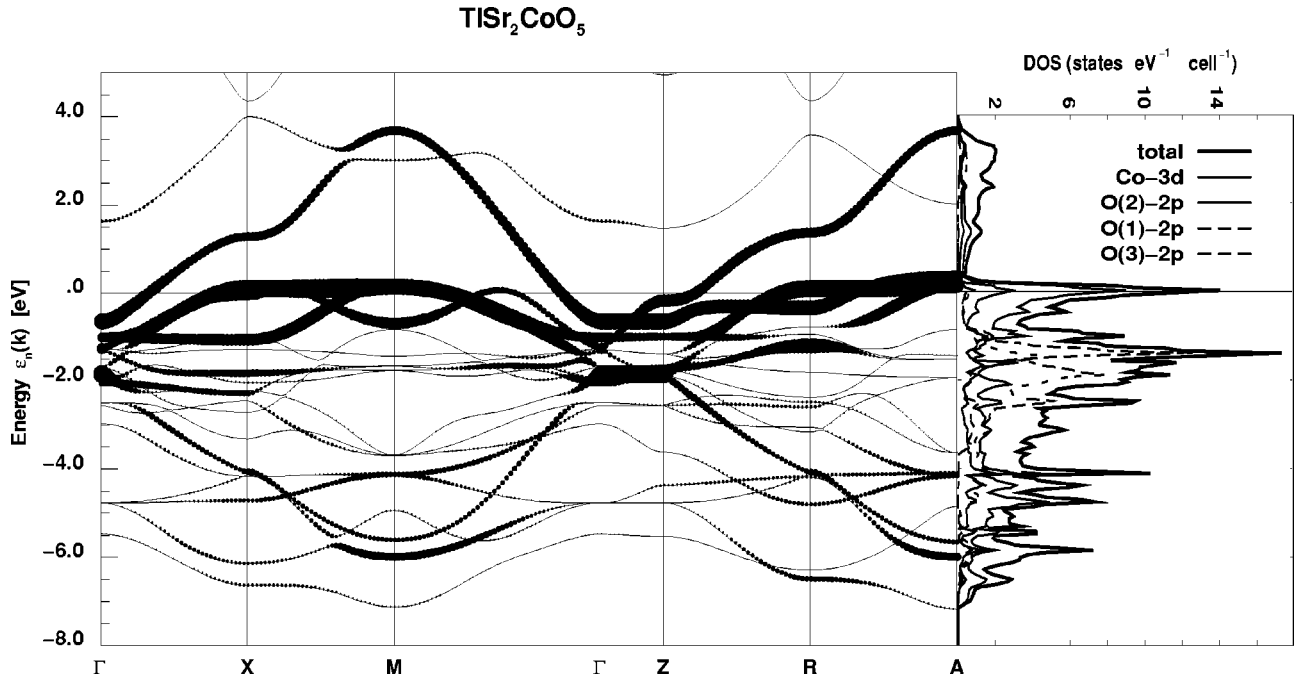

FIG. 4. Nonmagnetic LDA band structure of $TlSr_2CoO_5$. The relative cobalt $3d$ weight of the bands is symbolized via black dots in the band structure. For comparison we also included the DOS (see Fig. 2) at the right-hand side of the band structure. The broad line at the Fermi level between X and M is comprised of three bands (d_{xy}, d_{zx}, and d_{z^2}) which are nearly degenerate. The high-symmetry points are denoted as $\Gamma=(0,0,0)$, $X=(\pi/a,0,0)$, $M=(\pi/a,\pi/a,0)$, $Z=(0,0,\pi/c)$, $R=(\pi/a,0,\pi/c)$, and $A=(\pi/a,\pi/a,\pi/c)$.

ably well with the nonmagnetic LDA band structure of Fig. 4.

Concerning the values of the the crystal-field parameters, we note that, due to tetragonal symmetry, there is an exact degeneracy between the d_{zx} and d_{yz} orbitals in the LDA calculation. However, the values $\varepsilon_{xy}=-1.0$ and $\varepsilon_{zx/yz}=-0.5$ seem to violate ''standard lore,''[9] according to which the elongation of the octahedra in the z direction should shift d_{xy} to higher energies compared to $d_{zx/yz}$. One should note, however, that ε_i are approximately the energies at the Γ point, whereas the ''standard lore'' is valid in the ionic picture and would correspond, in our case, to the center of gravity of the different bands. Due to the larger bandwidth of the ''two-dimensional'' d_{xy} band in comparison with the ''one dimensional'' $d_{zx/yz}$ bands, the corresponding centers of gravity nearly coincide in Figs. 4 and 5. For the electronic structure of the metallic, ferromagnetic high-temperature phase of $TlSr_2CoO_5$, it is crucial that all three bands

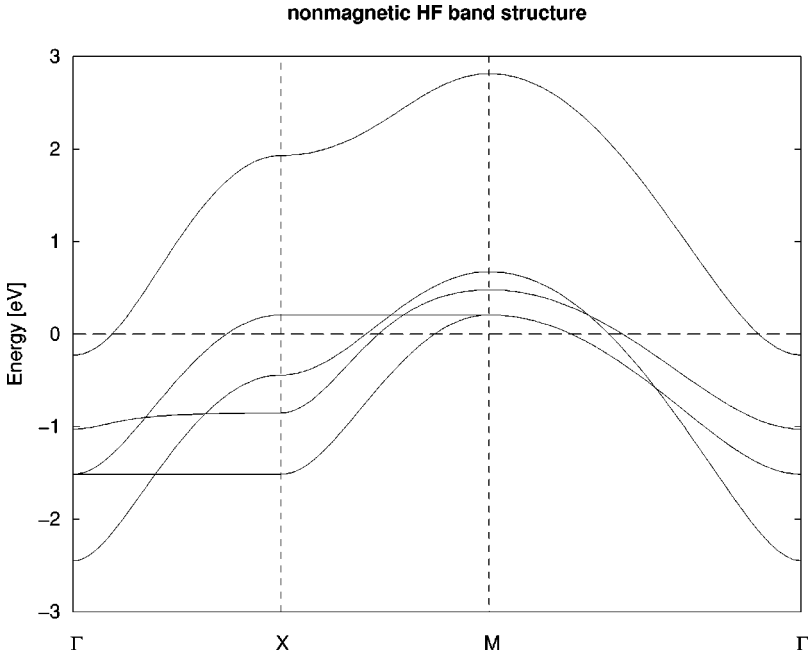

FIG. 5. Band structure of the nonmagnetic Hartree-Fock solution of a minimal tight-binding model of the CoO_2 plane. The notation of $\vec{k}$ points is as in Fig. 4.

TABLE I. Occupation numbers of various Hartree-Fock solutions of the minimal tight binding model.

Solution	Energy/meV		Occupation numbers						Magnetization/μ_B
			d_{xy}	d_{zx}	d_{yz}	d_{z^2}	$d_{x^2-y^2}$	sum	
Nonmagnetic	0	n_d	0.84	0.81	0.81	0.76	0.30	7.04	
Ferromagnetic	−653	$n_d^{\uparrow}$	1.00	1.00	1.00	0.98	0.63	4.61	2.41
		$n_d^{\downarrow}$	0.55	0.70	0.70	0.08	0.17	2.20	
Orbital order	−674	$n_{dA}^{\uparrow}$	1.00	1.00	1.00	0.98	0.67	4.65	2.52
		$n_{dA}^{\downarrow}$	0.69	0.89	0.29	0.09	0.17	2.13	
(quasistable)		$n_{dB}^{\uparrow}$	1.00	1.00	1.00	0.98	0.67	4.65	2.52
		$n_{dB}^{\downarrow}$	0.69	0.29	0.89	0.09	0.17	2.13	
Spin and	−720	$n_{dA}^{\uparrow}$	1.00	1.00	1.00	1.00	0.45	4.45	2.07
		$n_{dA}^{\downarrow}$	0.90	0.90	0.31	0.09	0.18	2.38	
orbital order		$n_{dB}^{\uparrow}$	1.00	1.00	1.00	0.99	0.91	4.90	3.11
		$n_{dB}^{\downarrow}$	0.37	0.28	0.88	0.09	0.17	1.79	

$\{d_{xy}, d_{zx/yz}\}$ cross the Fermi level, which is due to their widths being larger than their crystal-field splittings; see Fig. 4. It remains an open question, however, how the difference in dimensionality and width among the $\{d_{xy}, d_{zx/yz}\}$ bands affects the screening of the Coulomb interaction. This question was considered in detail[16] in the context of Sr_2RuO_4, another layered perovskite.

We now discuss the magnetic solutions of the HF approach. The homogeneous ferromagnetic solution (see Table I) is metallic, and 650 meV lower in energy than the nonmagnetic solution. The good agreement with the energy gain in the LDA (540 meV) and similar occupation numbers in the local-density and HF approximation indicate that our parameter assignment is satisfactory. Allowing for different occupations of d_{zx} and d_{yz} in a chess-board-like pattern, we find a metastable state with orbital order that decays into a ground state with both orbital and spin order, and which contains Co sites with two different configurations: $m_B = 3.11\mu_B$ (close to high spin) and $m_A = 2.07\mu_B$ (intermediate spin). This instability was signaled, in our calculation, by an energy gain of 67 meV due to combined orbital and spin order. The origin of the instability of the homogeneous ferromagnetic state is the orbital degeneracy of d_{zx} and d_{yz}, and the near degeneracy of intermediate- and high-spin configurations. This instability occurs in a rather large parameter region near values which were derived for $TlSr_2CoO_5$. However, due to the large dimensionality of the parameter space of our HF model [Eq. (2)], we did not perform a systematic study. In Fig. 6 we give the spectral density of the ferromagnetic state and of the two chess-board-like ordered states in a small region around the Fermi level. As we can see, any kind of order leads to a decrease of spectral density at the Fermi level, but only the orbital- and spin-ordered solution is insulating. This is also visible in the HF band structure (Fig. 7).

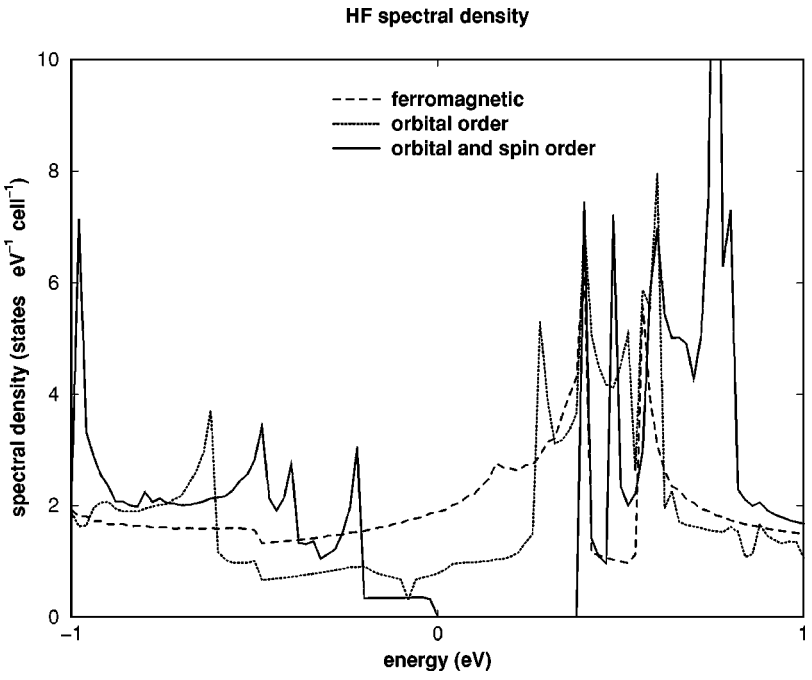

FIG. 6. Comparison of spectral weights for three magnetic Hartree-Fock solutions in the region ± 1 eV around the Fermi level (located at zero energy).

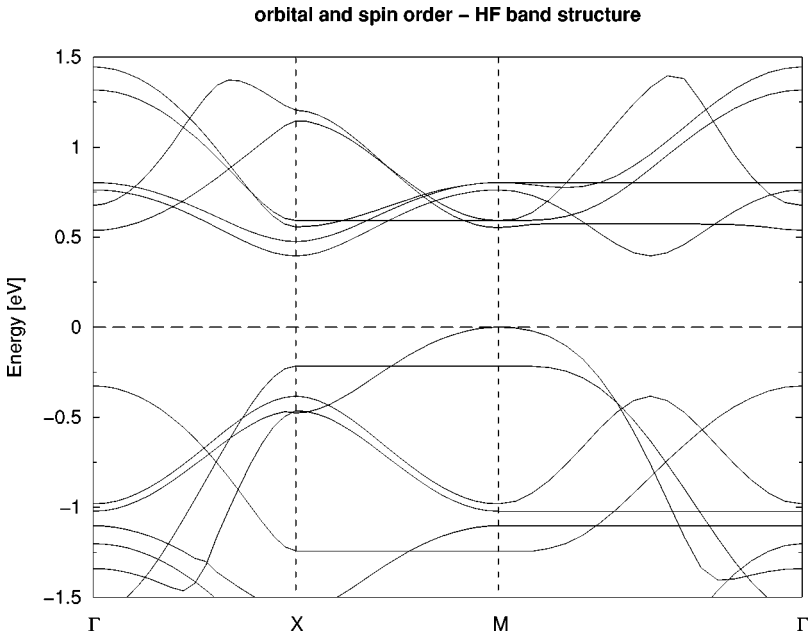

FIG. 7. Hartree-Fock band structure of the orbital- and spin-ordered solution of the minimal tight binding model.

It should be noted that the chess-board-like superstructure found here does not correspond to the orthorhombic low-temperature phase seen experimentally, with its 2:1 ratio of high- and intermediate-spin states.[3] We also investigated the experimental superstructure of the CoO_2 plane within the model Hartree-Fock approach, but found no solution with lower energy than that with chess-board order. The lattice degrees of freedom may have to be included into the model to obtain the correct pattern, because the nearest-neighbor Co-O distance for high spin is probably larger than the corresponding distance for intermediate spin [as can be concluded from the analogy with the famous Invar alloys Fe_xNi_{1-x} (Ref. 17)]. Another possibility is that next-nearest-neighbor interactions in an effective pseudospin model generate the experimentally observed pattern.[21] The present investigation of the electron system alone can only indicate the instability of the high-temperature phase, but it is not able to predict the correct low-temperature crystal structure.

INTERPRETATION OF RESULTS

We now interpret the results of our LDA and HF calculations in terms of a simplified model. As a first step, we recall that there is only $d \leftrightarrow p$ hopping, and neither direct $d \leftrightarrow d$ nor $p \leftrightarrow p$ hopping. This, and the fact that only cobalt d states are at the Fermi level, allows us to extract an effective $d \leftrightarrow d$ hopping by eliminating the oxygen orbitals in standard fashion,[18]

$$t_{dd'}^{eff}(\vec{a}) = \varepsilon_d \delta_{dd'} + \frac{t_{dp}(\vec{a}) t_{d'p}(-\vec{a})}{\Delta\varepsilon} = \varepsilon_d \delta_{dd'} - \frac{t_{dp}(\vec{a}) t_{pd'}(\vec{a})}{\Delta\varepsilon},$$

$$t_{dd'}^{eff}(\vec{x}) = \varepsilon_d \delta_{dd'} - \frac{1}{\Delta\varepsilon} \begin{pmatrix} {t_{t_{2g}}}^2 & 0 & 0 & 0 & 0 \\ 0 & 0 & 0 & 0 & 0 \\ 0 & 0 & {t_{t_{2g}}}^2 & 0 & 0 \\ 0 & 0 & 0 & \frac{1}{4}{t_{e_g}}^2 & -\frac{\sqrt{3}}{4}{t_{e_g}}^2 \\ 0 & 0 & 0 & -\frac{\sqrt{3}}{4}{t_{e_g}}^2 & \frac{3}{4}{t_{e_g}}^2 \end{pmatrix}, \tag{13}$$

where $\vec{a} \in \{\vec{x}, \vec{y}, -\vec{x}, -\vec{y}\}$ denotes the direction of hopping, and $\Delta\varepsilon$ is the offset between the Co and oxygen bands. Actually, due to the high degree of $d \leftrightarrow p$ hybridization the second order expression [Eq. (13)] is certainly not sufficient to provide correct numbers for $t_{dd'}^{eff}$, but nonetheless it should give the correct matrix structure. Just like the original hopping, the effective $t_{dd'}^{eff}$ is also anisotropic and orbitally dependent, with d_{zx} (d_{yz}) electrons hopping in the x y direction, and forming one-dimensional bands. Using the Coulomb energy of Eq. (7) this provides us with a simplified model that involves only d orbitals:

$$H = \sum_{d,s,\vec{R}} \varepsilon_d a_{d,s}^{\dagger}(\vec{R}) a_{d,s}(\vec{R}) + \sum_{d,d',\vec{R},\vec{R}',s} t_{dd'}^{eff}(\vec{R}-\vec{R}') \times a_{d,s}^{\dagger}(\vec{R}) a_{d',s}(\vec{R}') + \sum_{\vec{R}} j_H [D_{\vec{R}} - (\vec{s}_{tot,\vec{R}})^2] + \frac{u}{2} N_{\vec{R}}^2, \tag{14}$$

where j_H and u are renormalized values of J_H and $\tilde{U}$ due to the elimination of the oxygen orbitals. However, the precise

amount of renormalization is difficult to calculate, and is beyond the scope of the present discussion.

The above five-band model must be simplified further to extract the relevant degrees of freedom. We first note that the crystal-field parameters derived above are such that in the ionic case ($t_{dd'}^{eff}=0$) the three configurations of Fig. 8 are lowest in energy. We further highlight the orbitals closest to the Fermi level, which we believe to be itinerant by bold arrows. This suggests a minimal model with three itinerant-electron species, namely, $d_{x^2-y^2}^{\uparrow}$ and the two degenerate minority-spin bands $d_{zx}^{\downarrow}$ and $d_{yz}^{\downarrow}$. This physical picture is also supported by the ferromagnetic HF solution, where only $d_{x^2-y^2}^{\uparrow}$ is partly occupied among all the majority-spin bands, and the occupation of $d_{z^2}^{\downarrow}$ and $d_{x^2-y^2}^{\downarrow}$ in Table I is indeed small (the occupation of $d_{xy}^{\downarrow}$, however, deviates quite strongly from unity). The low-energy sector responsible for the metal-insulator and spin transition should be the competition between

$$\begin{aligned} s=1:&\quad xy\uparrow\downarrow,\ zx\uparrow\downarrow,\ yz\uparrow,\ 3z^2-r^2\uparrow \ \text{ or } \ x\leftrightarrow y,\\ s=2:&\quad xy\uparrow\downarrow,\ zx\uparrow,\ yz\uparrow,\ 3z^2-r^2\uparrow,\quad x^2-y^2\uparrow. \end{aligned} \tag{15}$$

In other words, $xy\uparrow\downarrow$ is only a spectator orbital, while $\{zx\uparrow,yz\uparrow,3z^2-r^2\uparrow\}$ provides a total spin of 3/2, and the exact degeneracy between d_{zx} and d_{yz} is kept as one of the driving mechanisms of the transition. The spin transition is then due to the competition between a down-spin electron $zx\downarrow$ or $yz\downarrow$ and an up-spin electron $x^2-y^2\uparrow$. Combining the spins of $\{zx\uparrow,yz\uparrow,3z^2-r^2\uparrow\}$ into an effective spin-3/2 degree of freedom, we can represent this competition as

$$\{S_{3/2}^{\uparrow},\ zx\downarrow\} \quad \text{or} \quad \{S_{3/2}^{\uparrow},\ yz\downarrow\}\Leftrightarrow\{S_{3/2}^{\uparrow},\ x^2-y^2\uparrow\}, \tag{16}$$

where we used Hund's coupling to exclude misaligned spins. To describe these qualitative ideas more precisely, we propose the model

$$\begin{aligned} H=&\varepsilon\sum_{\vec{R},s} a_{3,s}^{\dagger}(\vec{R})a_{3,s}(\vec{R})-\sum_{\vec{R},\vec{R}',s}\sum_{i=1}^{3} t_{ii}^{eff}(\vec{R}-\vec{R}')\\ &\times a_{i,s}^{\dagger}(\vec{R})a_{i,s}(\vec{R}')-2j_H\sum_{\vec{R}}\vec{S}_{\vec{R}}(\vec{s}_{\vec{R},3}-\vec{s}_{\vec{R},2}-\vec{s}_{\vec{R},1})\\ &+\frac{u}{2}\sum_{\vec{R},i,j} n_{\vec{R},i}n_{\vec{R},j}+j\sum_{\vec{R},\vec{R}'}\vec{S}_{\vec{R}}\cdot\vec{S}_{\vec{R}'} \end{aligned} \tag{17}$$

where the orbitals are numbered as $\{1,2,3\}\leftrightarrow\{zx,yz,x^2-y^2\}$, and t_{ii}^{eff} is an anisotropic and orbitally dependent hopping matrix. Model (17) is formulated in an extended phase space in comparison to Eq. (14), since $|S_{3/2}^{\uparrow},zx\uparrow\rangle$ and $|S_{3/2}^{\uparrow},yz\uparrow\rangle$ do not exist in the five-band model. But those unphysical states are at a high-energy, due to Hund's coupling j_H. The origin of the antiferromagnetic exchange coupling j should be the virtual superexchange of the singly occupied states that were excluded from our model; in addition, the coupling $\vec{S}_{\vec{R}}(\vec{s}_{\vec{R},3}-\vec{s}_{\vec{R},2}-\vec{s}_{\vec{R},1})$ makes sure that the spins of electrons in the orbitals $i=1$ and 2 are antiparallel to the spin 3/2 vector, and vice versa for $i=3$. A detailed estimate of the model parameters in Eq. (17) is beyond the scope of the present paper, but it is clear that we have to consider the range of parameters $u\gg j_H\gg\varepsilon,t,j$. The condition $j_H\gg t$ suppresses virtual hopping processes for antiparallel nearest-neighbor spins $\vec{S}_{\vec{R}}$, whereas they remain possible for parallel spins. In the limit of $j_H\gg\varepsilon,t$ the fermions are spin polarized; double occupation of the same orbital is automatically excluded by Fermi statistics, and we therefore dropped the local double-occupation D term in Eq. (17). The above model still admits high-energy processes (involving energy costs of u and j_H) that must be integrated out to obtain a true low-energy model.

To argue for the minimal model [Eq. (17)], we compare some of the possible two-site clusters in second-order perturbation theory (Fig. 9) (for simplicity, we use identical transfer amplitudes t, and restrict ourselves to leading terms). We see that for a ferromagnetic spin arrangement there is a competition between an orbitally ordered state $s=1$ (realized for $\varepsilon>t^2/u$) and a mixed orbital- and spin-ordered state ($\varepsilon<t^2/u$) which is also realized in the model HF approach. Next we see from the mixed-spin cluster in the figure that hopping processes are influenced by the relative spin orientation. In this cluster, there is a competition between ferromagnetic order favored by a gain in delocalization energy

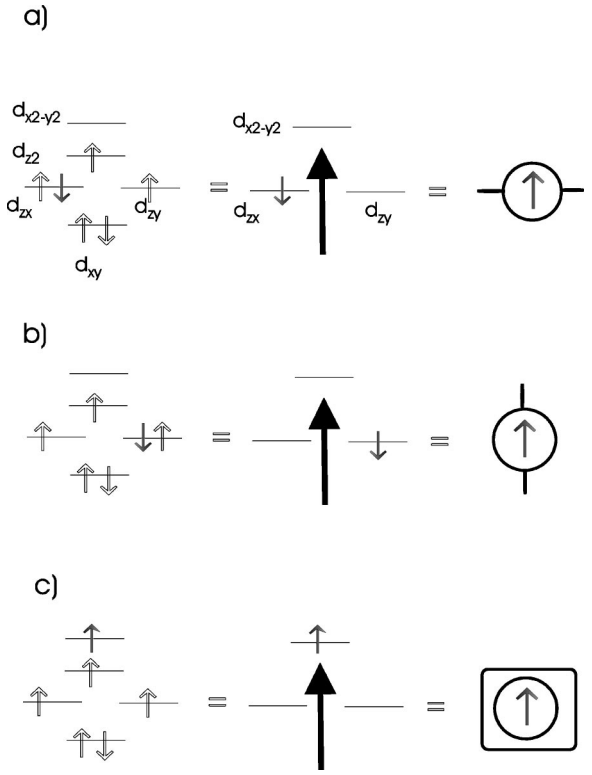

FIG. 8. The lowest ionic configurations of Co^{3+} in $TlSr_2CoO_5$ from the perspective of the CoO_2 plane in our simplified effective model. Configurations (a) and (b) correspond to intermediate spin states and are degenerate ($d_{zx}^{\downarrow},d_{yz}^{\downarrow}$), whereas configuration (c) is a high-spin state ($d_{x^2-y^2}^{\uparrow}$). The bold arrows correspond to itinerant states; the remaining states are localized, and are combined into an effectice spin 3/2 (middle row). The right row introduces a notation.

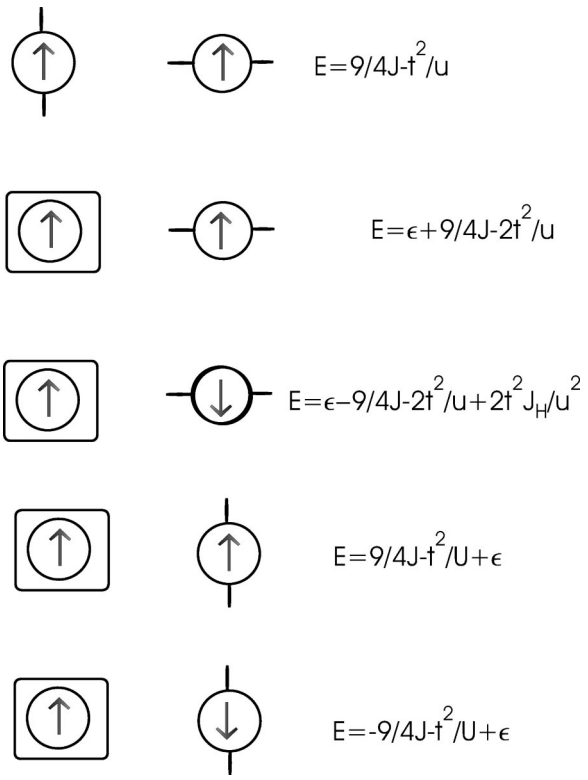

FIG. 9. Perturbation theory for configurations of a two-site cluster in the CoO_2 plane in the simplified effective model.

$\sim(t^2/u)(j_H/u)$ and antiferromagnetic order favored by a gain in magnetic energy $\sim j$. The ferromagnetic delocalization energy is expected to dominate j, and therefore neighboring high- and intermediate-spin states should order ferromagnetically (see Ref. 3) and it is easy to see that neighboring high-spin states ($s=2$) have an antiferromagnetic exchange in our simplified model [Eq. (17)].

There is a similarity between the model we propose here and the Zener double-exchange model,[19] except that our model has flipped spins for some of the orbitals to describe the spin transition, and we also have a total of three species of electrons per site at $j_H \gg t$. For sufficiently small values of u, there will be, by analogy with the double-exchange model, ferromagnetic and metallic phases, because charge transport is possible for parallel spin orientations, while for $u \to \infty$ the system is insulating. Thus we expect a rich phase diagram of this reduced model as a function of its parameters $\{\varepsilon, t, j_H, u, j\}$, with phases of mixed magnetic and orbital or spin order, and which may be metallic or insulating as a function of its parameters.

V. CONCLUSIONS

Using LDA band-structure calculations for the high-temperature tetragonal phase and a HF approach in a minimal model of the perovskite plane, we found states that are lower in energy than the homogeneous and ferromagnetic states. More specifically, we found that the homogeneous state is unstable toward orbital order and spin state disproportionation. We propose this instability to be the driving mechanism of the metal to insulator transition. A dynamical spin disproportionation above the transition temperature would be compatible with Mössbauer data on ^{57}Fe-doped $TlSr_2CoO_5$, that suggest the existence of two inequivalent magnetic sites.[20] Based on our calculations, we also proposed a simplified model with only three states per site at $j_H \gg t$, plus an extra spin of $S=\frac{3}{2}$, and which we argue to have a rich phase diagram as a function of its model parameters. After this paper was completed we were kindly informed by C. Michel of an oxide synthesized at Caen[22] that contains CoO_2 planes isostructural to the ones considered here.

ACKNOWLEDGMENTS

We are indebted to J.-P. Doumerc for many helpful and inspiring discussions on his data, to A. Villesuzanne for a comparison with his own band-structure results, and to D. Khomskii and M. Pouchard for useful criticism. H. R. acknowledges funding by an individual grant of ''Deutscher Akademischer Austauschdienst,'' T. P. and R. H. both acknowledge support as ''Professeur Invité, '' and D. F. was supported by ''Regensburg Graduiertenkolleg Komplexität in Festkörpern,'' IFW Dresden and ''Groupement de Recherche Oxydes Remarquables.'' CPTMB is ''Equipe Associée au CNRS ERS 2120.''

[1] M. Imada, A. Fujimori, and Y. Tokura, Rev. Mod. Phys. **70,** 1039 (1998); Y. Tokura and N. Nagaosa, Science **288**, 462 (2000); also see J. B. Goodenough, *Magnetism and the Chemical Bond* (Wiley, New York, 1963), p. 52.

[2] K.I. Kugel and D.I. Khomskii, Zh. Éksp. Teor. Fiz. **64**, 1429 (1973) [Sov. Phys. JETP **37**, 725 (1974)]; Usp. Fiz. Nauk **136**, 621 (1982) [Sov. Phys. Usp. **25**, 231 (1982)].

[3] M. Coutanceau, Doctoral Thesis, University of Bordeaux, 1996; J.-P. Doumerc, J.-C. Grenier, P. Hagenmuller, M. Pouchard, and A. Villesuzanne, J. Solid State Chem. **147**, 211 (1999); J. P. Doumerc, J. -C. Grenier, M. Coutanceau, A. Demourges, A. Villesuzanne, P. Dordor, and M. Pouchard (unpublished).

[4] W. Kohn, Rev. Mod. Phys. **71**, 1253 (1999).

[5] K. Koepernik and H. Eschrig, Phys. Rev. B **59**, 1743 (1999).

[6] V. I. Anisimov, F. Aryasetiawan, and A.I. Lichtenstein, J. Phys. C **9**, 767 (1997).

[7] T. Mizokawa and A. Fujimori, Phys. Rev. B **54**, 5368 (1996).

[8] A.P. Sutto, *Electronic Structures of Material* (Oxford University Press, Oxford, 1993); J.C. Slater and G.F. Koster, Phys. Rev. **94**, 1498 (1954). The Slater-Koster tables express the invariant tensor character of the overlap amplitudes.

[9] S. Sugano, Y. Tanabe, and H. Kamimura, *Multiplets of Transition Metal Ions In Crystals* (Academic Press, New York, 1970).

[10] B.H. Brandow, Adv. Phys. **26**, 651 (1977).

[11] A. Messiah, *Quantum Mechanics* (Wiley, New York, 1958), Vol. II.

[12] J. Hubbard, Proc. R. Soc. London, Ser. A **276**, 238 (1963); J. Kanamori, Prog. Theor. Phys. **30**, 275 (1963).
[13] N.D. Mermin, Ann. Phys. (N.Y.) **21**, 99 (1963).
[14] H. Rosner, R. Hayn, and J. Schulenburg, Phys. Rev. B **57**, 13 660 (1998).
[15] C.J. Ballhausen, *Introduction to Ligand Field Theory* (McGraw-Hill, New York, 1962).
[16] A. Liebsch and A. Lichtenstein, Phys. Rev. Lett. **84**, 1591 (2000).
[17] E.F. Wassermann, in *Ferromagnetic Materials*, edited by K.H.J. Buschow and E.P. Wohlfahrt (North-Holland, Amsterdam, 1990), Vol. 5, p. 237.
[18] P. Fulde, *Electron Correlations in Molecules and Solids*, Springer Series in Solid State Sciences Vol. 100 (Springer, Berlin, 1991), p. 289.
[19] C. Zener, Phys. Rev. **82**, 403 (1951); P.W. Anderson and H. Hasegawa, *ibid.* **100**, 675 (1955).
[20] J.-P. Doumerc, M. Coutanceau, L. Fournes, J.-C. Grenier, M. Pouchard, and A. Wattiaux, C.R. Acad. Sci., Ser. IIc: Chim 637 (1999).
[21] D. Khomskii (private communication).
[22] A.C. Masset, C. Michel, A. Maignan, M. Hervieu, O. Toulemonde, F. Studer, B. Raveau, and J. Hejtmanek, Phys. Rev. B **62**, 166 (2000).